

# Colloidal Electrostatic Interactions Near a Conducting Surface

Marco Polin and David G. Grier

*Department of Physics and Center for Soft Matter Physics,  
New York University, 4 Washington Place, New York, NY 10003*

Yilong Han

*Department of Physics and Astronomy, University of Pennsylvania, 209 South 33rd St., Philadelphia, PA 19104*

(Dated: March 23, 2022)

Charged-stabilized colloidal spheres dispersed in deionized water are supposed to repel each other. Instead, artifact-corrected video microscopy measurements reveal an anomalous long-ranged like-charge attraction in the interparticle pair potential when the spheres are confined to a layer by even a single charged glass surface. These attractions can be masked by electrostatic repulsions at low ionic strengths. Coating the bounding surfaces with a conducting gold layer suppresses the attraction. These observations suggest a possible mechanism for confinement-induced attractions.

Charge-stabilized colloidal spheres carrying the same sign charge and dispersed in deionized water are predicted to repel each other by the mean-field theory of macroionic interactions. This reasonable prediction has been repeatedly challenged by experimental observations that have been interpreted as evidence for like-charge colloidal attractions. Several methods have been introduced for probing these interactions directly, the most sensitive of which are based on digital video microscopy measurements of individual spheres' trajectories. When applied to dispersions of highly charged micrometer-scale spheres in deionized water, these techniques have indeed revealed anomalous long-ranged like-charge attractions in the effective pair potential [1, 2, 3, 4], but only when the spheres are rigidly confined to thin layers by charged glass surfaces [2, 4, 5]. Isolated pairs of spheres, by contrast, are found to repel each other in excellent agreement with standard theoretical predictions [2, 6, 7].

These observations have proved controversial, both because the effect has resisted explanation, and also because a host of experimental artifacts might have mimicked attractions in the published measurements. In the first place, like-charged colloidal attractions are inconsistent with the Poisson-Boltzmann mean-field theory for macroionic interactions [8, 9, 10, 11]. The observed attractions are too strong and long-ranged to be accounted for by van der Waals interactions [1, 12]. Efforts to explain the observations on the basis of other non-mean-field mechanisms have proved inconclusive or unsuccessful [13]. Simulations on smaller, simpler systems also have failed to reproduce the experimental observations.

Given the effect's apparent subtlety and the challenge it poses to basic notions in the field, ruling out experimental artifacts takes on particular importance. The introduction of thermodynamically self-consistent analytical tools [4, 14, 15] ensures that colloidal pair potentials extracted from trajectory data are free from such spurious effects as nonequilibrium kinematic coupling [16] and uncorrected many-body correlations [17]. These tests, however, cannot account for systematic errors in

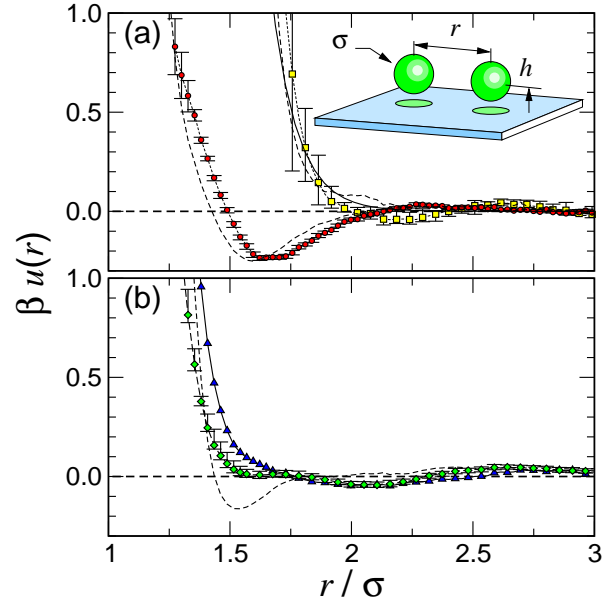


FIG. 1: Measured pair potentials  $u(r)$  for  $\sigma = 1.58 \mu\text{m}$  diameter silica spheres near a single wall ( $H \simeq 200 \mu\text{m}$ ). (a) Glass surface with  $\kappa^{-1} = 180 \pm 10 \text{ nm}$  (squares), showing monotonic repulsion, and  $\kappa^{-1} \approx 60 \text{ nm}$  (circles), displaying long-ranged attraction. Inset: schematic of the geometry. The solid curve is a fit to Eq. 4 with  $Z = 6500 \pm 1000$ . (b) Single gold-coated surface (diamonds) with  $\kappa^{-1} \approx 100 \text{ nm}$ . Potentials obtained with the HNC closure are plotted. Those obtained with the PY closure are indistinguishable. Dashed curves are uncorrected results. Correcting for imaging artifacts removes an apparent minimum in (b), but not in (a). The corrected pair potential is purely repulsive for a thin cell ( $H = 15 \mu\text{m}$ ) with two gold-coated surfaces (triangles).

the trajectory data themselves. Imaging artifacts that displace colloidal spheres' apparent centroids in digital microscopy images [18, 19] recently have been shown to mimic anomalous attractions at least under some circumstances [18]. Their discovery has therefore cast doubt on all previous reports of like-charge colloidal attractions.

This Letter presents experimental evidence for

anomalous confinement-induced like-charge colloidal attractions obtained with thermodynamically self-consistent distortion-corrected video microscopy measurements. Having confirmed the appearance of anomalous confinement-induced like-charge attractions under conditions comparable to those described previously, we further explore the role of surface properties in modifying colloidal electrostatic interactions. Previous studies have focused on the influence of pairs of closely spaced charged glass surfaces on the interactions between micrometer-scale spheres composed of polystyrene sulfate [1, 2, 3, 4], silica [4, 14, 15] and polymethyl methacrylate (PMMA) [20] dispersed in clean water. One exception is a study of PMMA spheres confined by neutral elastomer surfaces, in which the appearance of long-ranged attractions was ascribed to capillary forces [21]. We demonstrate that attractions between colloidal silica spheres in equilibrium can be induced even by a single charged glass wall, but are not by gold-coated surfaces under otherwise identical experimental conditions. These results are summarized in Fig. 1.

Our samples consist of uniform silica spheres  $\sigma = 1.58 \pm 0.06 \mu\text{m}$  in diameter (Duke Scientific Lot 24169) dispersed in deionized water and loaded into hermetically sealed sample volumes formed by bonding the edges of glass #1.5 coverslips to the surfaces of glass microscope slides separated by  $H = 200 \mu\text{m}$ . Access to the sample volume is provided by glass tubes bonded to holes drilled through the slides. Filling the tubes with mixed bed ion exchange resin maintains the ionic strength below  $5 \mu\text{M}$ , corresponding to a Debye-Hückel screening length of  $\kappa^{-1} \approx 200 \text{ nm}$ . Removing the ion exchange resin and allowing the dispersions to equilibrate with air reduces the screening length to  $\kappa^{-1} \approx 60 \text{ nm}$ . To investigate the influence of the bounding surfaces' properties on confined colloids' interactions, we coated the inner surfaces of some volumes with 10 nm gold films on 10 nm titanium wetting layers before assembly. These metallic films have a resistivity of  $50 \Omega/\square$  and are optically transparent. Sealed samples were mounted on the stage of a Zeiss Axiovert 100 STV microscope where they were allowed to equilibrate at room temperatures ( $T = 297 \pm 1 \text{ K}$ ). The dense silica spheres rapidly sediment into a monolayer with their centers about  $0.9 \mu\text{m}$  above the lower wall and with out-of-plane fluctuations smaller than  $300 \text{ nm}$  [4, 5]. The more distant wall is far enough from the sedimented spheres at the upper end of this range that we ascribe any anomalous effects to confinement by a single wall.

The bright-field imaging system provides a magnification of  $212 \text{ nm/pixel}$  on a Hitachi TI-11A monochrome charge coupled device (CCD) camera. The resulting video stream is recorded and digitized into 10 deinterlaced video fields per second, each of which is analyzed [22] to recover the single spheres' centroids, typically identified to within  $1/10$  pixel.

Individual spheres' images extend beyond their bright

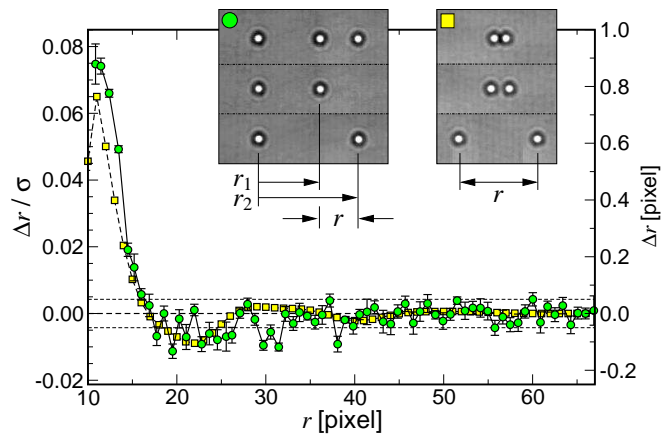


FIG. 2: Measurement of the imaging artifact due to overlap of single-sphere light scattering patterns. Circles represent data obtained with holographic optical tweezer measurements and squares with computer-generated composite images.

centers with alternating dark and bright diffraction fringes, which are far-field projections of the micrometer-scale particles' light scattering patterns [23, 24]. When two particles are close enough for their visible scattering patterns to overlap, the distortions induced in their individual images cause systematic deviations in the spheres' measured separations [18]. These non-monotonic separation-dependent deviations can affect the qualitative form of the inter-particle pair potential estimated from measured particle positions, in some cases creating the appearance of long-ranged attractions when none exist [18]. Fortunately, this effect can be measured, and the measurements used to correct the derived results [18].

Figure 2 shows two complementary approaches for measuring this imaging artifact, one of which can be applied *a posteriori* to archival data. In the first, holographic optical tweezers [25, 26] are used to trap three colloidal spheres in a line. One sphere is held far enough from the other two to avoid any distortions, and is used as a reference. The two other traps are set at a fixed separation and filled with particles, first one at a time, and then together. The apparent positions,  $r_1$  and  $r_2$ , of these spheres relative to the reference particle are measured [22] both with and without the neighbor. The difference between the spheres' true separation,  $r = r_2 - r_1$ , and the apparent separation when both traps are filled is a measurement of the distortion  $\Delta r$ , which is plotted as a function of true separation in Fig. 2. As previously reported [18], these deviations substantially exceed the quoted error bound for single-particle tracking [22] at separations relevant for colloidal interaction measurements.

The optical trapping method must be performed *in situ* and thus cannot be applied to the data in previously published studies [1, 2, 3, 4, 14, 15]. Equivalent results can be obtained by analyzing images of single

isolated spheres, and so can be applied after the fact. Digitally translating a copy of such an image and superimposing it on the original yields a composite image of known separation, equivalent to the incoherent superposition of two single-particle scattered fields. Examples are shown in the second inset to Fig. 2. The apparent separation in each composite can be measured as before, and the difference between this and the known separation is a measurement of the separation-dependent deviation. As shown in Fig. 2, the results agree well for the spheres in our studies. The successful comparison with the direct optical tweezer measurement confirms this method's accuracy, and it is used in the following measurements.

We estimate a confined dispersion's effective pair potential by amassing data on equilibrium pair separations over periods of roughly one hour [5], with temperature fluctuations maintained below  $\pm 1^\circ\text{C}$ . Time-resolved particle distribution data then are distilled into the radial distribution function,

$$g(r) = \frac{1}{n^2} \langle \rho(\mathbf{r}' + \mathbf{r}, t) \rho(\mathbf{r}, t) \rangle \quad (1)$$

where  $n = N/A$  is the areal density of  $N = \langle N(t) \rangle$  particles in the field of view of area  $A$ ,  $\rho(\mathbf{r}, t)$  is the instantaneous particle distribution at time  $t$ , and the averages are over angles and time. To assess the influence of separation-dependent imaging artifacts we analyzed both  $g(r)$  and the result obtained by approximately correcting for systematic separation distortions,  $\tilde{g}(r) = g(r + \Delta r) (1 + \frac{d}{dr} \Delta r)$ . Our samples are dilute enough that higher-order many-body distortions have a negligibly small effect.

Estimates for the effective pair potential can be extracted from  $g(r)$  and  $\tilde{g}(r)$  in either the hypernetted-chain (HNC) or Percus-Yevick (PY) approximations as [5, 27]

$$\beta u(r) = -\ln g(r) + \begin{cases} nI(r) & \text{(HNC)} \\ \ln(1 + nI(r)) & \text{(PY)} \end{cases} \quad (2)$$

where  $\beta^{-1} = k_B T$  is the thermal energy scale, and where the convolution integral

$$I(r) = \int_A [g(r') - 1 - nI(r')] [g(|\mathbf{r}' - \mathbf{r}|) - 1] d^2 r' \quad (3)$$

is solved iteratively, starting with  $I(r) = 0$ . The results then can be tested for thermodynamic self-consistency using previously reported methods [14, 15].

Typical results for silica spheres near glass and gold-coated surfaces are plotted in Fig. 1(a) and (b) respectively. Uncorrected data are plotted as dashed curves in Fig. 1, and corrected results as discrete points.

Imaging artifacts have little influence on the data in Fig. 1(a). Colloidal silica spheres hovering over a single charged glass surface at low ionic strength repel each

other, in agreement with previously reported measurements [4, 5, 14]. The purely monotonic pair potentials obtained under these conditions also agree with predictions of mean-field theory [28],

$$\beta u(r) = Z^{*2} \lambda_B \frac{\exp(-\kappa r)}{r}, \quad (4)$$

where  $Z^* = Z \exp(\kappa\sigma/2)/(1 + \kappa\sigma/2)$ , is the spheres' effective charge number, where the Bjerrum length,  $\lambda_B = \beta e^2/(4\pi\epsilon_0\epsilon) = 0.717$  nm, sets thermal range for electrostatic interactions in a medium of dielectric constant  $\epsilon$ , and where the Debye-Hückel screening length  $\kappa^{-1}$  sets the range over which electrostatic interactions are screened by the concentration  $c$  of (monovalent) ions. The fit charge number  $Z = 6500 \pm 1000$  is consistent with previous measurements on similar spheres [5], even after correcting for imaging artifacts. The fit screening length  $\kappa^{-1} = 180 \pm 10$  nm corresponds to  $c = \kappa^2/(4\pi\lambda_B) = 5.7$   $\mu\text{M}$ .

Qualitatively different results are obtained when the ionic strength is allowed to increase to roughly 50  $\mu\text{M}$  (Fig. 1(a, circles)). Under these circumstances, the measured pair potential has a minimum 0.2  $k_B T$  deep at a center-to-center separation of 2.7  $\mu\text{m}$  ( $1.7\sigma$ ), even after correcting for imaging artifacts. Unlike previous reports of attractions induced by pairs of closely spaced glass walls [1, 2, 3, 4, 14], the data in Fig. 1(a) suggest that even a single surface suffices to induce a long-ranged attraction between nearby pairs of spheres. This is qualitatively consistent with the observation that the repulsion between a pair of charged colloidal spheres is diminished by introducing a third sphere into their vicinity [29], with the charged wall in our experiment playing the role of the third sphere.

Reanalyzing data from Refs. [4] and [14] with the *a posteriori* correction method also confirms the presence of anomalous attractions in more tightly confined charge-stabilized dispersions. Furthermore, the increasing prominence of the attractive component of the interaction with decreasing wall separation [4] appears to have been correctly interpreted as intrinsic properties of the inter-particle pair potential. The attraction's apparent dependence on ionic strength also recalls a similar trend observed in the earliest report of the effect [1].

Imaging artifacts play a more striking role for the data in Fig. 1(b, diamonds). In this case, an apparent minimum in the uncorrected pair potential disappears entirely after accounting for overlapping images. The absence of an attraction is noteworthy because the data in Figs. 1(a, circles) and (b, diamonds) were obtained under comparable conditions of ionic strength, the only difference being the gold coating on the bounding surface in (b). A comparable result is obtained for a thin sample ( $H = 15$   $\mu\text{m}$ ) where both surfaces are gold-coated (Fig. 1(b, triangles)). Reducing the inter-wall separation in bare glass cells generally has been found to strengthen

wall-induced attractions [2, 4]. These observations therefore suggest that nominally uncharged gold surfaces do not induce anomalous attractions under conditions for which charged glass surfaces do.

Confirming the importance of surface charge in confinement-induced attractions helps to narrow the possible explanations for the effect. A growing body of calculations show that large, highly charged colloidal spheres can induce non-monotonic correlations in the distribution of simple ions, not captured by mean-field theory, even in 1:1 electrolytes [30, 31, 32], and that these can mediate effective inter-particle attractions. Related calculations suggesting that bounding charged walls also induce such correlations between *pairs* of spheres [33, 34] have proved controversial [10, 35, 36], although they appear to be consistent with numerical simulations [37]. These excess correlations correspond to departures from local electroneutrality in the electrolyte surrounding the macroions. Under some conditions, they tend to inject extra counterions between pairs of spheres, thereby inducing an effective attraction. Modeling this diffuse space charge as a point charge,  $q$ , at the midpoint between the spheres' centers suggests an effective pair potential [38]

$$\beta u(r) = Z^* \lambda_B \left( Z^* \frac{\exp(-\kappa r)}{r} + 4q \frac{\exp(-\kappa r/2)}{r} \right), \quad (5)$$

which agrees well with measured results, such as those in Fig. 1. The solid curves in Fig. 1(a) are both consistent with  $q = 10 \pm 5$ . Those in Fig. 1(b) are consistent with  $q = 0$ . In the latter case, the nominally uncharged walls would have no excess counterions to contribute.

This semi-heuristic space charge model demonstrates that correlation-induced attractions beyond the mean-field approximation can be masked by long-ranged electrostatic repulsions in systems at very low ionic strength. Less efficient deionization at small wall separation might then explain why wall-induced attractions have been observed [4] for wall spacings as large as  $H = 30 \mu\text{m}$ , but not previously for  $H \gtrsim 200 \mu\text{m}$  [4, 5].

This work was supported by the donors of the Petroleum Research Fund of the American Chemical Society.

---

[1] G. M. Kepler and S. Fraden, Phys. Rev. Lett. **73**, 356 (1994).  
 [2] J. C. Crocker and D. G. Grier, Phys. Rev. Lett. **77**, 1897 (1996).  
 [3] M. D. Carbajal-Tinoco, F. Castro-Román, and J. L. Arauz-Lara, Phys. Rev. E **53**, 3745 (1996).  
 [4] Y. Han and D. G. Grier, Phys. Rev. Lett. **91**, 038302 (2003).  
 [5] S. H. Behrens and D. G. Grier, Phys. Rev. E **64**, 050401(R) (2001).  
 [6] J. C. Crocker and D. G. Grier, Phys. Rev. Lett. **73**, 352 (1994).

[7] K. Vondermassen, J. Bongers, A. Mueller, and H. Versmold, Langmuir **10**, 1351 (1994).  
 [8] J. E. Sader and D. Y. C. Chan, J. Colloid Interface Sci. **213**, 268 (1999).  
 [9] J. C. Neu, Phys. Rev. Lett. **82**, 1072 (1999).  
 [10] E. Trizac and J.-L. Raimbault, Phys. Rev. E **60**, 6530 (1999).  
 [11] J. E. Sader and D. Y. C. Chan, Langmuir **16**, 324 (2000).  
 [12] B. A. Pailthorpe and W. B. Russel, J. Colloid Interface Sci. **89**, 563 (1982).  
 [13] A. Gopinathan, T. Zhou, S. N. Coppersmith, L. P. Kadanoff, and D. G. Grier, Europhys. Lett. **57**, 451 (2002).  
 [14] Y. Han and D. G. Grier, Phys. Rev. Lett. **92**, 148301 (2004).  
 [15] Y. Han and D. G. Grier, J. Chem. Phys. **122**, 064907 (2005).  
 [16] T. M. Squires and M. P. Brenner, Phys. Rev. Lett. **85**, 4976 (2000).  
 [17] M. Brunner, C. Bechinger, W. Strepp, V. Lobaskin, and von Grunberg. H. H., Europhys. Lett. **58**, 926 (2002).  
 [18] J. Baumgartl, J. L. Arauz-Lara, and C. Bechinger, preprint (2005).  
 [19] J. Baumgartl and C. Bechinger, Europhys. Lett. **71**, 487 (2005).  
 [20] J. C. Crocker, Ph.d., University of Chicago (1996).  
 [21] B. Cui, B. Lin, S. Sharma, and S. A. Rice, J. Chem. Phys. **116**, 3119 (2002).  
 [22] J. C. Crocker and D. G. Grier, J. Colloid Interface Sci. **179**, 298 (1996).  
 [23] C. F. Bohren and D. R. Huffman, *Absorption and Scattering of Light by Small Particles* (Wiley Interscience, New York, 1983).  
 [24] B. Ovaryn and S. H. Izen, J. Opt. Soc. America **17**, 1202 (2000).  
 [25] E. R. Dufresne and D. G. Grier, Rev. Sci. Instr. **69**, 1974 (1998).  
 [26] M. Polin, K. Ladavac, S.-H. Lee, Y. Roichman, and D. G. Grier, Opt. Express **13**, 5831 (2005).  
 [27] E. M. Chan, J. Phys. C **10**, 3477 (1977).  
 [28] W. B. Russel, D. A. Saville, and W. R. Schowalter, *Colloidal Dispersions*, Cambridge Monographs on Mechanics and Applied Mathematics (Cambridge University Press, Cambridge, 1989).  
 [29] C. Russ, M. Brunner, C. Bechinger, and H. H. Von Grunberg, Europhys. Lett. **69**, 468 (2005).  
 [30] R. Hastings, J. Chem. Phys. **68**, 675 (1978).  
 [31] B. P. Lee and M. E. Fisher, Europhys. Lett. **39**, 611 (1997).  
 [32] M. D. Carbajal-Tinoco and P. Gonzalez-Mozuelos, J. Chem. Phys. **117**, 2344 (2002).  
 [33] D. Goulding and J.-P. Hansen, Mol. Phys. **95**, 649 (1998).  
 [34] D. Goulding and J.-P. Hansen, Europhys. Lett. **46**, 407 (1999).  
 [35] E. M. Mateescu, Phys. Rev. E **64**, 013401 (2001).  
 [36] E. Trizac and J. L. Raimbault, Phys. Rev. E **64**, 043401 (2001).  
 [37] E. Allahyarov, I. D'Amico, and H. Löwen, Phys. Rev. E **60**, 3199 (1999).  
 [38] D. G. Grier and Y. Han, J. Phys.: Condens. Matt. **16**, S4145 (2004).